


Modeling the Dynamic Power-to-Gas Process: Coupling Electrolysis with CO₂ Methanation

Bjarne Kreitz^{1,2*}, Jörn Brauns¹, Gregor D. Wehinger^{1,2}, and Thomas Turek^{1,2}

DOI: 10.1002/cite.202000019

 This is an open access article under the terms of the Creative Commons Attribution-NonCommercial-NoDerivs License, which permits use and distribution in any medium, provided the original work is properly cited, the use is non-commercial and no modifications or adaptations are made.



Supporting Information
available online

The dynamic operation of a power-to-gas plant powered by wind energy is theoretically studied by coupling an empirical model of an alkaline water electrolyzer with a 1D heterogeneous model of a methanation reactor. H₂ produced by the electrolyzer follows the wind power profile, but operation in the part-load range can raise safety concerns. The dynamically generated methane quality comes close to the required value for injection into the gas grid, if the stoichiometric ratio is controlled. To satisfy the gas quality at all times, it is necessary to design a more tolerant reactor.

Keywords: Alkaline water electrolysis, Dynamic operations, Methanation, Power-to-gas, Process modeling

Received: February 10, 2020; *revised:* June 15, 2020; *accepted:* July 15, 2020

1 Introduction

Producing methane with the power-to-gas (PtG) process is a promising technology to tackle the demand for long-term energy storage and a sustainable natural gas economy. In this process, H₂, produced by renewable energies, is used to hydrogenate CO₂ in the methanation reaction [1]. A trend for PtG is the development of small-scale container-based units for decentralized energy storage applications. These units usually consist of an alkaline water electrolyzer (AEL) for the production of H₂ owing to low investment and maintenance costs as well as a high lifetime [2]. Due to the limited space, an intensified reactor is required in terms of heat and mass transfer, e.g., a microstructured reactor. Improved temperature control is possible with this reactor type and, thus, higher operating temperatures can be applied without exceeding the critical catalyst temperature. Microstructured reactors are also investigated for other power-to-X processes such as Fischer-Tropsch [3,4] and methanol [5] synthesis. Fig. 1 shows a schematic overview of the PtG process with possible CO₂ sources. The container-based setup enforces space restrictions on the PtG unit, which may result in an intended dynamic operation to reduce the space and costs for intermediate electricity (battery) or H₂ (buffer tank) storage.

Directly powering an AEL with a wind turbine results in a dynamic operation owing to the fluctuating nature of the wind velocity. Wind power is often favored over solar photovoltaic power because of no daytime-limited availability [2]. The intermittent load variations in the electrolyzer can not only cause an irregular hydrogen flow but rather raise concerns about process safety. Gas impurities based on

crossover mechanisms can demand a safety shutdown of the unit, which is critical for low current densities. H₂ and O₂ form explosive mixtures between 4 and 96 vol % foreign gas contamination. Therefore, alkaline water electrolyzers perform a safety shutdown when reaching 50 % of the lower explosion limit. The main gas contamination is caused by electrolyte mixing, which transfers dissolved product gas species into the other half-cell [6,7]. The H₂ impurities in O₂ are limiting since the product ratio is 2:1.

Methanation reactors are usually designed for a steady-state operation while considering constraints such as a specified conversion and maximum catalyst temperature. The strongly exothermic CO₂ methanation is generally conducted in a wall-cooled reactor, with a polytropic temperature profile, accompanied by a distinct hot spot formation at the entrance of the reactor. A previous study showed that even a microstructured reactor exhibits severe temperature and conversion changes under forced periodic operation [8]. This is not only caused by the reaction kinetics, but also by

¹Bjarne Kreitz, Jörn Brauns, Prof. Dr.-Ing. Gregor D. Wehinger,

Prof. Dr.-Ing. Thomas Turek

kreitz@icvt.tu-clausthal.de

Institute of Chemical and Electrochemical Process Engineering, Clausthal University of Technology, Leibnizstraße 17, 38678 Clausthal-Zellerfeld, Germany.

²Bjarne Kreitz, Prof. Dr.-Ing. Gregor D. Wehinger,

Prof. Dr.-Ing. Thomas Turek

Research Center Energy Storage Technologies (EST), Clausthal University of Technology, Am Stollen 19A, 38640 Goslar, Germany.

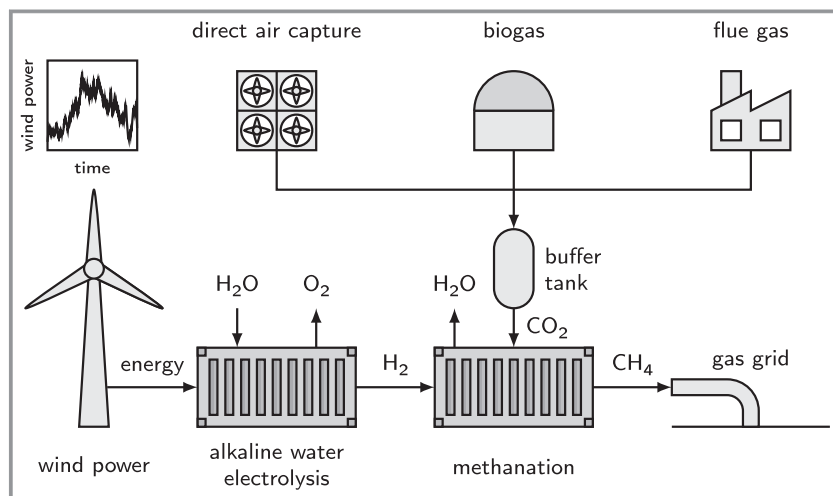


Figure 1. Schematic of the power-to-gas process with possible carbon sources.

variations in the transport properties of the varying composition of the gas mixture.

Within this study, process modeling is used to investigate the behavior of the PtG setup when a real wind power profile is applied. The following questions are to be answered by the simulation:

- How does the electrolyzer react to an irregularly shaped input signal (H_2 production, process safety)?
- How does the methanation reactor behave (catalyst temperature, CH_4 concentration)?

Two operation scenarios of the methanation reactor are studied: an uncontrolled dynamic operation with solely varying the H_2 inlet flow rate and a controlled operation with a constant H_2/CO_2 ratio.

2 Methods

2.1 Input Profile

A real wind power signal of a weather station located in Clausthal-Zellerfeld, Germany, is used to modulate the input of the AEL, which is depicted in Fig. 2a. An exemplary day is arbitrarily chosen and the data of the input signal is reported in the Supporting Information (SI). High-frequency oscillations, as well as a superimposed low-frequency oscillation, can be seen with drastic variations in the amplitude of the wind power profile. The wind velocity profile has a mean value of 1.8 m s^{-1} . The maximum positive velocity deviation is 182 % of

the mean value, while the lowest velocity amounts to 21 %.

The wind velocity profile is normalized to the average and used to define two scenarios for powering an AEL, which is shown in Fig. 2b. The nominal operation point of the AEL is fixed at 3 kA m^{-2} , which is in the range of typical current densities. In the high load scenario, this is defined as the nominal load and corresponds to 100 %. In the low load case, the AEL is operated at an average load of a third of the nominal value, which is 1 kA m^{-2} . These cases are chosen to show the different system behaviors of AEL powered by renewable energies.

2.2 Alkaline Water Electrolysis

Various approaches with different complexity can describe the system behavior of alkaline water electrolyzers. While physically reasonable models are setup-independent since system dimensions can be defined by the required input parameters, empirical correlations are only valid for the actual electrolyzer system [2]. Often, the parameters for physically reasonable models are challenging to quantify and the development of such models is a recent research topic [7]. Therefore, empirical correlations are used in this study to gain exemplary insights into the dynamic behavior of the AEL.

The produced H_2 flow rate is calculated by Faraday's law and is thereby directly proportional to the current density. Next to the H_2 production rate, cell voltage and gas impuri-

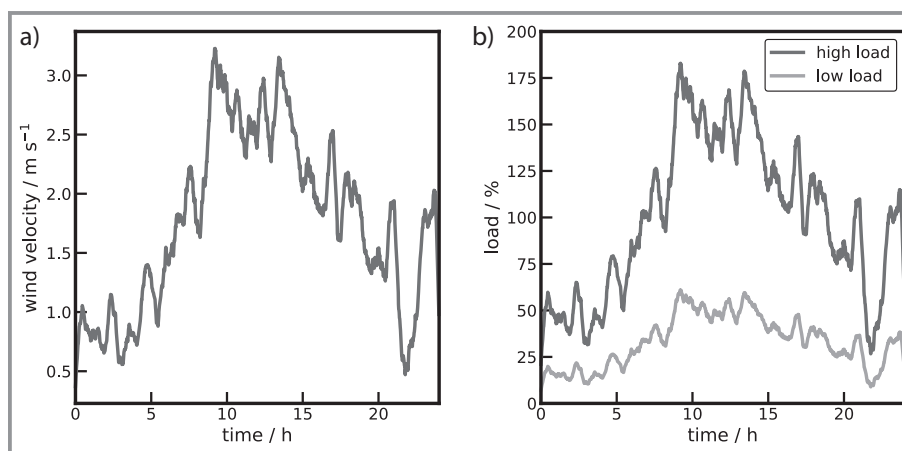


Figure 2. a) Time-related wind velocity profile measured by the weather station in Clausthal-Zellerfeld, Germany and b) two different operation scenarios derived from the wind profile. While high power availability is favored, a power shortage with a low load scenario can occur during times with a limited abundance of wind power. 100 % load corresponds to the designated steady-state current density of 3 kA m^{-2} .

ty are significant parameters of interest for AELs. Hence, both variables are calculated by empirical correlations depending on current density, temperature, pressure, and electrolyte concentration [9, 10]. The efficiency of AELs is mainly influenced by the required cell voltage and gas impurity. Furthermore, the system pressure and the temperature have to be taken into account. While the atmospheric operation requires a less expensive construction, the pressurized operation is preferred to avoid a cost-intensive mechanical compression [2]. Therefore, this study focuses on a pressurized operation at 9 bar to provide the required pressure for the methanation. The suitable operation temperature for AELs is between 50 and 80 °C depending on the electrolyte concentration due to a maximum of the electrolyte conductivity. With a temperature of 60 °C and an electrolyte concentration of 32 wt% KOH, typical operation conditions are assumed [11]. For details on the equations, refer to the SI.

2.3 Methanation

A dynamic 1D heterogeneous model, as described in our previous work [8], is used to model the methanation reactor, which is only briefly explained here. The reactor is designed based on a rippled-plate heat exchanger design with alternating cooling and reaction channels. The reaction channels are filled with a spherical Ni/Al₂O₃ catalyst with a diameter of 400 μm and a thermal oil is used as a cooling medium. One simulated channel has dimensions of 2 × 2 mm with a length of 40 cm to achieve a sufficient conversion during the steady-state operation. The reactor is operated at an inlet temperature of 280 °C, which is also the temperature of the cooling medium, an inlet pressure of 8 bar, and a gas hourly space velocity (GHSV) of 3143 h⁻¹. A Langmuir-Hinshelwood-Hougen-Watson reaction rate expression from Koschany et al. [12] is used for the CO₂ methanation kinetics on a Ni/Al₂O₃ catalyst. This reaction rate expression is developed from steady-state experiments and, therefore, may not be able to capture dynamic phenomena correctly [13]. However, transient kinetic approaches are not available at the moment.

The reactor is designed for the steady-state operation with constraints, such as a pressure drop below 0.4 bar m⁻¹, a hot spot temperature below 550 °C, and a methane concentration in the dry exhaust gas above 90 vol%, to fulfill the German gas net regulations for low calorific gas (L-gas) quality. The model of the microstructured reactor is implemented in gPROMS and solved with a Runge-Kutta method.

For the dynamic operation of the methanation reactor, the average flow rate of the transient signal is adjusted to the steady-state value to enable a fair comparison. Throughout this study, it is assumed that the CO₂ input signal can be controlled and is not affected by irregular variations. Therefore, a buffer tank is included in Fig. 1. However, the CO₂ inlet flow can also be subjected to fluctuations in reality, which is neglected to reduce complexity. Two cases are regarded in the present simulation study, which are an uncontrolled dynamic operation (Case I) and a controlled dynamic operation (Case II).

In the first case, it is assumed that only the H₂ signal is subjected to fluctuations due to the AEL, while the volumetric flow rate of CO₂ is kept constant. For Case I, the reactor is subjected to changes in the inlet flow rate as well as the inlet composition. A more realistic scenario is represented in Case II, where a controlled dynamic operation is applied. The CO₂ flow rate is adjusted so that a stoichiometric feed composition is maintained, which can be achieved by a simple control system. The H₂ flow rate is the same as in Case I and only the total flow rate varies over time.

3 Results and Discussion

3.1 Alkaline Water Electrolysis

The results of cell voltage and gas impurity are shown in Fig. 3 for both load scenarios. While the reversible cell voltage at atmospheric conditions is around 1.2 V at a system temperature of 60 °C, the operation at a pressure of 9 bar significantly increases this value to approximately 1.27 V due to the higher energy demand for gas bubble formation. Obviously, the low load scenario also requires a lower cell voltage compared to the high load case in Fig. 3a. In general, the calculated cell voltages are in agreement with expected values of around 1.6 and 2.1 V [2].

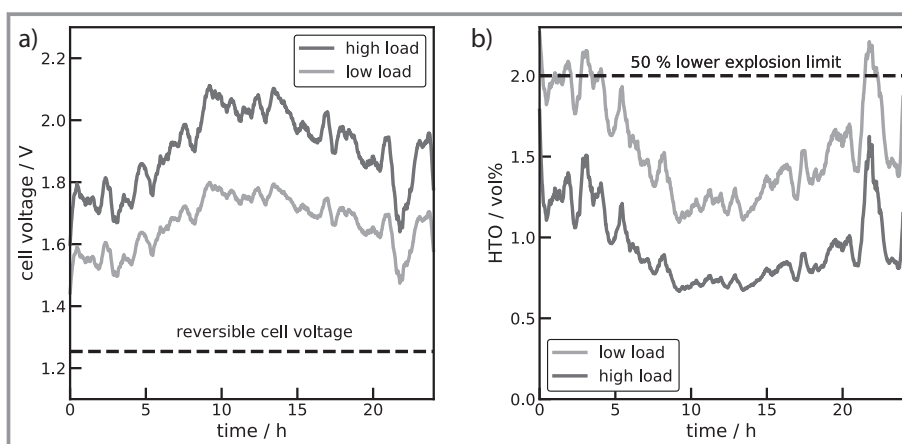


Figure 3. Results of the empirical model for both load scenarios. a) Cell voltage of the AEL and b) H₂ content in anodic O₂ (HTO) at a system temperature of 60 °C and a pressure of 9 bar.

The difference in cell voltage for atmospheric and pressurized operation is negligible since the increase of the reversible cell voltage is compensated by lower ohmic losses of gas bubbles due to decreasing bubble diameters at elevated pressures. The resulting gas contamination of H₂ in O₂ is shown in Fig. 3b. While the gas impurity is always higher for the low load scenario, both profiles show similar results. When the AEL is operated in the part-load range significantly below 20 % of its nominal load, the safety limit of 2.0 vol % is reached and suitable safety strategies are necessary [6, 7, 11]. However, this simulation study does not include the event of a safety shutdown since only small overruns of the safety limit occur. While the low load scenario shows a gas impurity between 1.2 and 2.1 vol %, the H₂ content is in the range of 0.7 to 1.7 vol % for the high load case. Therefore, an operation above the part-load range is favorable since fewer safety problems may occur.

As the H₂ production is directly proportional to the applied current density, it is also directly proportional to

the wind profile as well (see SI). Hence, the fluctuations are not damped by the AEL and the small losses due to the oxidation of H₂ with O₂ in the oxidizer can be neglected.

3.2 Methanation

The steady-state concentration of methane in the dry exhaust gas for the designed operation point is 90.97 vol %, which is close to the equilibrium value at these conditions of 91.99 vol %, and the maximum gas-phase temperature is 431 °C. Fig. 4a shows the signal of the H₂ and CO₂ inlet volumetric flow rate for the applied wind profile. The oscillations of the H₂ inlet signal are identical to the wind velocity profile, with the same minimum and maximum load. A low volumetric flow rate and a low H₂/CO₂ ratio are present at the beginning of the signal and for Case I. The reactor is operated at an increased load between 7 and 19 h, with a maximum load of 182 % at 9.2 h.

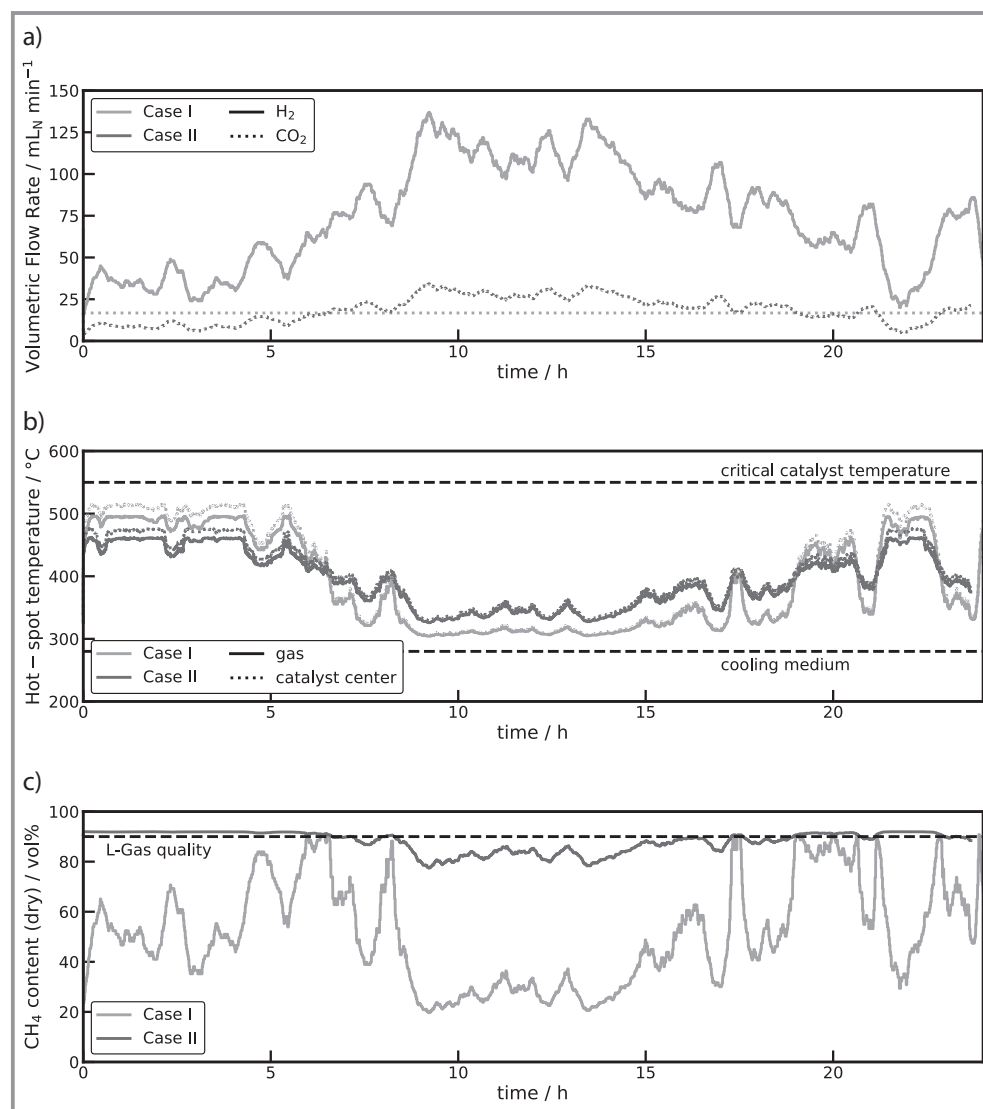


Figure 4. Temporal profiles for the investigated scenarios of a) volumetric inlet flow rate of H₂ (solid) and CO₂ (dotted). Please note that the H₂ inlet flow rate is identical in both scenarios. b) Hot spot temperature of the gas (solid) and catalyst center (dotted) and c) CH₄ content in the dry exhaust gas.

Temperature and concentration changes occur almost instantaneously compared to the time scale of the fluctuations, which means that the input frequency and the output frequency are nearly equal. A new steady-state is reached within 15 s, as a consequence of the low thermal inertia of a single channel [8]. This would be different in a stack of several hundreds of these channels, which cannot be described by the model used in this study.

The temporal hot spot temperature profile is presented in Fig. 4b. For low flow rates and high CO₂ contents in the feed, high temperatures of up to 500 °C are obtained when the ratio is not adjusted. Some studies report a lower critical catalyst temperature of 500 °C than the one assumed in this study, which is already surpassed at the beginning for Case I [14, 15]. Although this temperature is specific for a catalytic system and the simulation results are only qualitative, it still clearly shows that the maximum steady-state temperature can be exceeded during the transient operation. An increasing flow rate and H₂ concentration result in a decrease in the hot spot temperature due to the higher velocity. This is amplified by the larger thermal conductivity of H₂ and the improved overall heat transfer coefficient, respectively. It has been confirmed for Case I that the varying reactant ratio does not violate the validity range, for which the kinetic expression was developed (see SI). A nearly constant hot spot temperature with a low value of 310 °C for Case I and 330 °C for Case II is obtained between 8 and 15 h of the wind profile, despite large fluctuations in the H₂ inlet signal. Comparing the temperatures at the beginning of the signal for the variable and stoichiometric feed ratio, it can be seen that the maximum temperatures are lower for the stoichiometric case. This is caused by the enlarged thermal conductivity of the mixture, despite the decreased overall heat transfer coefficient due to the lower flow rate [8]. A higher volumetric flow rate decreases the hot spot temperature by increasing the heat transfer in the packed bed and a lower conversion is the result because of a suppressed hot spot.

The temperature in the center of the catalyst is higher because of the exothermic reaction and the limited heat conductivity of the porous support (Al₂O₃). The maximum temperature difference between the catalyst center and the gas phase in the steady-state operation amounts to 10.7 K. A maximum difference of 18.4 K occurs for Case I and 13.8 K for Case II. This clearly shows that a heterogeneous model is required to accurately describe the transient methanation, which is also pointed out by Fischer et al. [16]. This difference decreases with increasing volumetric flow rate, which improves the heat removal from the catalyst and, thereby, lowers the hot spot temperature and the reaction rate.

Fig. 4c shows the methane concentration in the dry exhaust gas after the removal of water. With the variable H₂/CO₂ ratio, the methane concentration suffers from substantial variations. This is either caused by insufficient H₂ supply in the under-stoichiometric regime or H₂ excess in the over-stoichiometric composition. As a result, a purifica-

tion step or a recycle loop [17] for the unconverted reactants is required. The methane concentration meets the specified value for the L-gas quality during the first 6 h for Case II. After this time, the increasing volumetric flow rate lowers the residence time in the reactor, which means that the conversion decreases and methane is not produced in the required purity. This effect is amplified by a decreased thermal resistance in the catalyst bed, enabling a more efficient heat transfer that reduces the hot spot temperature and the reaction rate, respectively.

The simulation shows that a simple adjustment of the CO₂ inlet flow rate is not enough to ensure a constant L-gas quality of the produced methane. Further control strategies or an improved reactor design are required to achieve the desired conversion over a broad range of operating conditions. These technologies need to ensure safe operation in terms of the maximum temperature at the hot spot and the gas quality. Possible control methods are the adjustment of the coolant temperature [14, 16], the design of a tolerant catalyst [15], or a tolerant reactor [18]. A tolerant reactor refers to a reactor that can meet the required specification even for varying operating conditions. Such reactors can be designed by taking possible variations into account during the optimization problem [18].

4 Conclusion

The effect of a real wind power signal on a PtG unit is investigated through the coupling of an AEL model with a model for a methanation reactor. While for the AEL, only a simple model is used in this study, the microstructured methanation reactor is described by a detailed 1D heterogeneous model.

The H₂ production by the AEL directly follows the oscillations of the input profile, without any delay. Therefore, the cell voltage and the gas impurity define the efficiency during the transient operation. While a low load also results in low cell voltages, the gas impurity is significantly increased below 20 % of the nominal load. Suitable strategies may be required to avoid safety shutdowns.

The simulation of the methanation reactor shows that the modulation of the H₂ inlet signal leads to vigorous variations in methane concentration and hot spot temperature. The temperature profile is nearly the same for both investigated cases, with the profile of Case II showing a lower amplitude. However, a product gas with L-gas quality is produced for some hours with the stoichiometric inlet composition. Deviations from the L-gas quality arise from the low residence time and the low temperature at the hot spot for too high flow rates. This study shows that it is necessary to adapt the design of the PtG plant either by a more tolerant reactor or by adding a purification step.

The transient operation of the PtG process will be further experimentally investigated by combining a lab-scale AEL with a fixed-bed methanation reactor. This can be used to

investigate operation modes of the AEL to guarantee safe operation even in a low load range and to study the transient kinetics of the CO₂ methanation experimentally.

Supporting Information

Supporting Information for this article can be found under DOI: <https://doi.org/10.1002/cite.202000019>.

This work is funded by the Deutsche Forschungsgemeinschaft (DFG, German Research Foundation), project numbers: 290019031, 391348959. Part of this work is supported and financed by Clausthal University of Technology, project Catalytic and Microbial Methanation as Basis for Sustainable Energy Storage (CliMb). We thank the Institute of Electrical Information Technology (IEI) of Clausthal University of Technology for sharing the weather data. Open access funding enabled and organized by Projekt DEAL. [Correction added on August 19, 2020, after first online publication: Projekt Deal funding statement has been added.]

References

- [1] M. Götz, J. Lefebvre, F. Mörs, A. McDaniel Koch, F. Graf, S. Bajohr, R. Reimert, T. Kolb, *Renewable Energy* **2016**, *85*, 1371–1390. DOI: <https://doi.org/10.1016/j.renene.2015.07.066>
- [2] J. Brauns, T. Turek, *Processes* **2020**, *8* (2), 248. DOI: <https://doi.org/10.3390/pr8020248>
- [3] M. Loewert, J. Hoffmann, P. Piermartini, M. Selinsek, R. Dittmeyer, P. Pfeifer, *Chem. Eng. Technol.* **2019**, *42* (10), 2202–2214. DOI: <https://doi.org/10.1002/ceat.201900136>
- [4] R. Güttel, T. Turek, *Energy Technol.* **2016**, *4* (1), 44–54. DOI: <https://doi.org/10.1002/ente.201500257>
- [5] H. J. Venvik, J. Yang, *Catal. Today* **2017**, *285*, 135–146. DOI: <https://doi.org/10.1016/j.cattod.2017.02.014>
- [6] P. Haug, M. Koj, T. Turek, *Int. J. Hydrogen Energy* **2017**, *42* (15), 9406–9418. DOI: <https://doi.org/10.1016/j.ijhydene.201612.111>
- [7] P. Haug, B. Kreitz, M. Koj, T. Turek, *Int. J. Hydrogen Energy* **2017**, *42* (24), 15689–15707. DOI: <https://doi.org/10.1016/j.ijhydene.2017.05.031>
- [8] B. Kreitz, G. D. Wehinger, T. Turek, *Chem. Eng. Sci.* **2019**, *195*, 541–552. DOI: <https://doi.org/10.1016/j.ces.2018.09.053>
- [9] M. Sánchez, E. Amores, L. Rodríguez, C. Clemente-Jul, *Int. J. Hydrogen Energy* **2018**, *43* (45), 20332–20345. DOI: <https://doi.org/10.1016/j.ijhydene.2018.09.029>
- [10] M. Hammoudi, C. Henaou, K. Agbossou, Y. Dubé, M. Doumbia, *Int. J. Hydrogen Energy* **2012**, *37* (19), 13895–13913. DOI: <https://doi.org/10.1016/j.ijhydene.2012.07.015>
- [11] P. Trinke, P. Haug, J. Brauns, B. Bensmann, R. Hanke-Rauschenbach, T. Turek, *J. Electrochem. Soc.* **2018**, *165* (7), F502–F513. DOI: <https://doi.org/10.1149/2.0541807jes>
- [12] F. Koschany, D. Schlereth, O. Hinrichsen, *Appl. Catal., B* **2016**, *181*, 504–516. DOI: <https://doi.org/10.1016/j.apcatb.2015.07.026>
- [13] B. Kreitz, J. Friedland, R. Güttel, G. D. Wehinger, T. Turek, *Chem. Ing. Tech.* **2019**, *91* (5), 576–582. DOI: <https://doi.org/10.1002/cite.201800191>
- [14] J. Bremer, K. Sundmacher, *React. Chem. Eng.* **2019**, *4* (6), 1019–1037. DOI: <https://doi.org/10.1039/C9RE00147F>
- [15] R. T. Zimmermann, J. Bremer, K. Sundmacher, *Chem. Eng. J.* **2020**, *387*, 123704. DOI: <https://doi.org/10.1016/j.cej.2019.123704>
- [16] K. L. Fischer, M. R. Langer, H. Freund, *Ind. Eng. Chem. Res.* **2019**, *58* (42), 19406–19420. DOI: <https://doi.org/10.1021/acs.iecr.9b02863>
- [17] S. Matthischke, S. Rönsch, R. Güttel, *Ind. Eng. Chem. Res.* **2018**, *57* (18), 6391–6400. DOI: <https://doi.org/10.1021/acs.iecr.8b00755>
- [18] J. Maußner, C. Dreiser, O. Wachsen, H. Freund, *J. Adv. Manuf. Process.* **2019**, *1* (3), e10024. DOI: <https://doi.org/10.1002/amp2.10024>